

General Disclaimer

One or more of the Following Statements may affect this Document

- This document has been reproduced from the best copy furnished by the organizational source. It is being released in the interest of making available as much information as possible.
- This document may contain data, which exceeds the sheet parameters. It was furnished in this condition by the organizational source and is the best copy available.
- This document may contain tone-on-tone or color graphs, charts and/or pictures, which have been reproduced in black and white.
- This document is paginated as submitted by the original source.
- Portions of this document are not fully legible due to the historical nature of some of the material. However, it is the best reproduction available from the original submission.

X-612-68-416
PREPRINT

NASA TM X- 63385

LOW ENERGY ELECTRON PRECIPITATION PATTERN AT HIGH LATITUDES

R. A. HOFFMAN

FACILITY FORM 602

N 69-10508
(ACCESSION NUMBER)
99
(PAGES)
TMX-63385
(NASA CR OR TMX OR AD NUMBER)
13
(CODE)
13
(CATEGORY)

NOVEMBER 1968



GSEFC

— GODDARD SPACE FLIGHT CENTER —
GREENBELT, MARYLAND

**LOW ENERGY ELECTRON PRECIPITATION PATTERN
AT HIGH LATITUDES**

R. A. Hoffman

November 1968

**GODDARD SPACE FLIGHT CENTER
Greenbelt, Maryland**

ABSTRACT

From a consideration of all data available to date from satellite-borne detectors measuring low energy electrons, an electron precipitation pattern at very high latitudes for periods of relatively low magnetic activity is formulated. From midnight through the dawn side until at least local noon, auroral oval latitudes are characterized by a broad, structureless precipitation, with the electrons having a hard energy spectrum and a pitch angle distribution which is almost isotropic over the upper hemisphere. Poleward of this region, although somewhat overlapping and apparently at all local times, there is a region of bursts or spikes of electrons with usually a very soft energy spectrum. At pre-midnight times highly structured electron precipitation occurs with rapidly varying spectra. Very little precipitation is observed near the magnetic pole.

INTRODUCTION

Data from charged particle detectors capable of measuring fluxes of electrons whose energies are below 10 kev indicate that there exists a region of precipitation of these low energy electrons poleward of the auroral oval near local noon and midnight in addition to the usual precipitation of higher energy electrons in the auroral oval. The Lockheed group, (Johnson et.al., 1966; Sharp and Johnson, 1967) with two short-lived satellite flights in 1963 and 1965, observed on the day side two distinct regions of precipitating electrons with characteristic differences in both the spectra and angular distributions. The higher latitude region was composed of soft electrons in intense structures and generally anisotropic pitch angle distributions. More recently results in a preliminary report from the Rice University satellite Aurora 1 indicate that the spacecraft transit across the high-latitude boundary of the auroral zone is nearly always evidenced by a sudden spectral softening and the onset of pronounced spatial or temporal anisotropy (Burch, 1968).

Data received from the low energy Auroral Particles Experiment aboard the OGO-4 satellite show that the high latitude region of soft electrons is composed of bursts of electrons, rather than being a region of broad, structured precipitation, and that this burst region occurs at most local times besides near the noon-midnight meridian.

EXPERIMENT

A detailed description of the Auroral Particles Experiment appears elsewhere (Hoffman and Evans, 1967). It contains an array of eight detectors, each comprised of an electrostatic analyzer and a channel electron multiplier. The results presented here are obtained primarily from two detectors while operated in their electron detection mode. These detectors always point radially away from the earth, and therefore in the high latitude region measure particles with pitch angles near 0° . They have bandpasses centered around 0.7 kev and 7.3 kev, with half widths of +19% and -13% of the center energy, and angular response of about $\pm 3^\circ$ by $\pm 7^\circ$. The geometric factor of each detector is about $6 \times 10^{-5} \text{ cm}^2\text{-ster}$ at the peak of the energy bandpass.

Pulses from the two detectors are accumulated into logarithmic accumulators over precisely the same time interval, a half a main telemetry frame, and then are blanked out for the other half of a frame. However, for simplicity of presentation data from the detectors will be plotted in the accompanying figures as time continuous histograms.

Counting rates from the detectors will be shown in counts/readout rather than converting them to fluxes, in order to display the counting statistics, especially for the plots containing high time resolution data or short accumulation times. Three telemetry bit rates are available from the spacecraft, 4, 16 and 64 kilobits/second, so each plot indicates the bit rate for the data acquisition. To convert the counting rates to fluxes the conversion factors are listed in

Table 1. Note that the factor for the 0.7 kev detector is about ten times that for the 7.4 kev detector because the latter samples a ten times wider differential energy slice.

SATELLITE ORBIT

The satellite was launched on July 28, 1967, into a low altitude polar orbit having an apogee of 908 km, a perigee of 412 km, an inclination of 86°, and an injection into a dawn-dusk orbital plane. Precession of the orbit due to this inclination together with the motion of the earth around the sun cause a change in local time of the orbital plane of about 1½° per day.

DATA EXAMPLES

The first data example is presented in Figure 1, a dusk to dawn pass very early in the life of the satellite. The data are averaged over eight accumulation periods. Extremely small fluxes were measured at invariant latitudes below 75° in the late afternoon hours. Poleward of this point was a region of precipitation characterized by rapid variations in the counting rates from the detectors and generally a soft electron energy spectrum. Fluxes exceeding 10^8 electrons/cm²-sec-ster-kev at 0.7 kev began at 78° and continued over the entire polar region, abruptly ending on the dawn side at 79°. This high latitude region of precipitation was initially observed in the quick look data received from the experiment during the early revolutions of the satellite in this dusk to dawn meridian, and was designated a "burst region" (Hoffman and Evans, 1968). The term "burst" was chosen as merely a subjective description of the appearance of the data and

is not meant to imply that the counting rate fluctuations are believed to be necessarily temporal in nature.

The burst region was followed by a broad band of rather structureless precipitation in the morning hours, extending as far south at 69° .

This pass showed an enormous burst of 7.3 kev electrons just after 0619 U.T. when the satellite was at a very high latitude at local noon. This very unusual burst contained some $30 \text{ ergs/cm}^2\text{-sec}$ of energy influx in the bandpass of the 7.3 kev detector alone, assuming reasonable isotropy over the upper hemisphere.

An example of a late morning pass with fluxes perhaps slightly larger than normal is shown in Figure 2. The data plotted are averaged over 40 accumulation periods. While data from all eight detectors in the experiment were almost entirely free from noise for several weeks after launch, a noise problem suddenly appeared in the outputs of several detectors, including the 0.7 kev detector, but not the 7.3 kev detector. The counting rates from the 0.7 kev detector plotted in the figures have this steady noise level subtracted, unless otherwise indicated.

For this pass a region of precipitation commenced at an invariant latitude of about 69° and was characterized by small variations in the counting rates and a relatively hard spectrum. (Note on the plot the 7.3 kev detector rate is displaced a decade lower than the 0.7 kev detector rate.) A four point electron energy spectrum obtained at 70° for these precipitated particles is shown in Figure 3 with the label "Band."

At about 73° the 0.7 kev detector counting rate suddenly increased and displayed rapid variations. The electron energy spectrum also became softer. Thus the region below 73° is equated to the low latitude morning band of the previously illustrated pass, and the region above 73° is considered to correspond to the burst region. In this example the two regions overlap from 73° to 75° , rather than separate so clearly as on the previous example.

The non-averaged data from the 0.7 kev detector during several of the bursts around 2103 U.T. are shown in Figure 4. The average spectrum for the large burst at about 2103:05 is shown in Figure 3 with the label "Burst." Note that the main difference between the two spectrums in the figure is the flux at 0.7 kev.

An example of a very early morning pass is shown in Figure 5. The data plotted are averaged over 64 accumulation periods. Again a region of harder, less structured precipitated fluxes is evident at latitudes less than 69° , whereas north of this latitude the very soft bursts are apparent.

This pass is especially interesting because it is one of the few acquired at the 64 kbps bit rate during the first half year of satellite operation. An example of this high resolution data from the 0.7 kev detector appears in Figure 6. This eight seconds of data begins with several bursts and ends in the region of the quiet band. Note the sharpness of each edge of the burst occurring at 0214:50.7 U.T., especially the trailing edge, where the counting rate drops by a factor of $3\frac{1}{2}$ in 18 milliseconds, or a distance traversed by the spacecraft of about

135 meters. The total width of the burst is only 0.25 seconds, during which the spacecraft traveled 2000 meters. Because the spectrum is as least as steep as that for the burst shown in Figure 3 for energies below 2.3 kev, it is impossible to realistically calculate the total energy input. However, the energy input measured solely by the 0.7 kev detector, assuming reasonable isotropy over the upper hemisphere, is about 5 ergs/cm²-sec. (However, see discussion below about pitch angle distributions.)

Data from a short segment of a pre-midnight pass are shown in Figure 7. This 16 kbps data is averaged over eight accumulation periods. This picture differs from the previous ones in that there is not as clear a delineation between the band and burst regions, if indeed a band is discernable. Rather the bursts extend almost to the southern limit of all precipitation, while the 7.3 kev electron precipitation occurs in a structured pattern. This pass is typical of others through the pre-midnight region.

SURVEY OF PRECIPITATION PARAMETERS

The precipitation of low energy electrons at high latitudes may be classified into two regions of precipitation, each with greatly different characteristics in temporal and/or spatial variations, energy spectrums and pitch angle distributions.

1. Temporal and/or Spatial Variations.

It becomes apparent from considering the data at the end of revolution 54 at about 08 hours MLT (Fig. 1), the beginning of revolution 1099 at 10 hours

MLT (Fig. 2), and the end of revolution 743 at 03 hours MLT (Fig. 5) that the precipitation occurring at lowest invariant latitudes is relatively structureless when compared with the precipitation occurring at higher latitudes. The positions of this "band" radiation from the revolutions illustrated are indicated in the polar plot of Figure 8 as heavy, solid bars beside the orbit loci.

The bursts of radiation lie poleward of the bands, and somewhat overlapping, which is especially evident in Figure 2 from 2101 to 2101:40 U.T. The locations of these bursts are illustrated in Figure 8 by a dashed bar beside the orbit. There is no evidence available to date to differentiate between a temporal or spatial nature of the bursts. Note especially from the high time resolution Figures 4 and 6 that the bursts are fairly isolated events: that the radiation levels between maxima are at or near background noise, or at least one or two orders of magnitude lower than the maxima.

In the pre-midnight region, the precipitation does not display this two region pattern, but rather there seems to appear only a burst region of generally harder radiation. At dusk at least during the days around revolution 54, there were neither bursts nor an appreciable band below about 75°.

To compare these observations with previous measurements we first plot in Figure 8 the locations of the "hard" and "soft" precipitation regions reported by Sharp and Johnson (1967) (curves labeled "L"). Near noon a detector sampling a differential energy interval near 1 kev was used to define the "center of gravity" of the highly structured region with a soft energy spectrum. For the hard day

region, a detector with an electron energy threshold of about 9 kev was used.

Thus these detectors would measure radiation whose characteristics should be similar to the 0.7 kev and 7.3 kev detectors primarily used in our study.

On the night side, at about 23 hours MLT apparently the two regions were not distinguishable, and the center of gravity of the nightside precipitation was defined based upon the response of a detector with an electron low energy threshold of 15 ev. However, in this region its counting rate pattern showed similar characteristics as the pattern from our 0.7 kev detector, in spite of its extremely low energy threshold.

Note that the Lockheed hard and soft zones lie in similar latitudinal ranges as the band and burst regions distinguished on revolutions 1099 and 54 on the day side, while in the pre-midnight region, a different precipitation pattern appears in both the Lockheed and our data.

The primary criteria used by Burch (1968) to separate his "Auroral Zone" from the "Soft Zone" was the energy spectrum, especially a comparison of the measurements below 2.4 kev and above 6.2 kev, as well as rapid variations in intensity. The locations of his two zones are also indicated on Figure 8 for the three passes whose data are published (Curves labeled "A" in the figure). The band and burst regions are obviously synonymous to his auroral and soft zones for the noontime pass. Comparing Burch's Figure 3, containing a pass crossing the midnight meridian at 71° latitude, with his other two figures containing the post-midnight and noontime passes, it is noticed that it is becoming more difficult to

distinguish between the two zones at this time. Burch points out that the rapid intensity variations in the lowest energy channel begin at a latitude below that of spectral softening.

Over the pole there appears to be a hole in the precipitation pattern with flux levels one or two orders of magnitude lower than in the burst region. (Burch, 1968; The more complex distribution pattern in the midnight region reported in Hoffman (1968) was compiled using geographic local time. The use of MLT indicates a single region over the pole relatively free of radiation.)

2. Energy Spectrums

The analysis of energy spectrums in the two dayside regions by Sharp and Johnson (1967) shows over an order of magnitude difference in the average energy between the band and burst regions. Burch's (1968) three point spectrums and our four point band and burst spectrums in Figure 5 indicate a great softening in the burst region compared with the band region. However, because the fluxes in the burst region are so highly variable, and the bursts may appear almost monoenergetically (e.g. the burst at 7.3 kev during revolution 54 at 0619, Figure 1), it is impossible to derive a "typical" burst spectrum.

Spectrums from the pre-midnight period are more difficult to classify. Sharp and Johnson (1967) indicate an "average" energy in the range 5 to 10 kev, intermediate between the two dayside zones. Burch (1968) continues his two zone concept, although the difference between the auroral and soft zones is not as striking as on the day side. From the data in Figure 7 we can obtain a wide

variety of spectrums in the range of invariant latitudes from 66° to 71° . At 66° , it would be extremely soft, while at $68\frac{1}{2}^\circ$ it would be typical of the daytime band. Again at 71° it would be comparable to soft daytime burst spectrums.

3. Pitch Angle Distributions

Pitch angle measurements obtained by these various experiments do not seem to organize into a consistent picture. Burch's (1968) measurements were made from a spinning satellite, making it almost impossible to distinguish between temporal and/or spatial variations and pitch angle anisotropies, especially in the soft zone.

The Lockheed data are usually presented as scatter plots of total energy fluxes for electrons with energies greater than 80 ev at about 56° pitch angle versus those near 0° pitch angle. In general in all radiation zones their data indicate anisotropies having maximum intensity at the larger pitch angle, with a tendency toward isotropy, especially at high flux levels. However, the soft day zone is less isotropic than the hard day zone.

In Figure 9, the four point pitch angle measurement in the morning band from 0622:27 to 0623:04 U.T. during revolution 54 (Figure 1) shows very nearly an isotropic distribution of 2.3 kev electrons, in spite of the fact that the detectors at the three smallest local pitch angles were measuring electrons in the loss cone. The variation in flux from 0° to 90° was only $\pm 10\%$ of the average flux, but does indicate a monotonically increasing flux with increasing pitch angle.

On the other hand, in the burst region our data contradict the Lockheed results. The bursts whose pitch angle distributions we have observed at 2.3 kev only have generally been isotropic, with a significant percentage displaying a field-aligned component with maximum intensity directed towards the atmosphere (Hoffman and Evans, 1968; Hoffman, 1968). We find no evidence for a pitch angle distribution with maximum intensity normal to the field lines.

4. Summary

Thus it appears that the Lockheed "hard zone," Burch's "Auroral Zone," and our "band" region are synonymous, as well as the "soft zones" of Lockheed and Burch and our "burst" region.

DISCUSSION

From a consideration of all the low energy electron data published to date, the following pattern of precipitation of electrons at high latitudes seems to be emerging for periods of relatively low magnetic activity:

- At latitudes more typical of the usual auroral oval, from midnight through the dawn side until at least local noon, there is a region of broad, relatively structureless precipitation. The pitch angle distributions are usually quite isotropic, though with a tendency for higher intensities at larger pitch angles, and the electrons have a relatively hard energy spectrum.
- Poleward of this region, although at times somewhat overlapping, and apparently at all local times, there is a region of bursts of electrons,

with usually very steep energy spectrums, but with pitch angle distributions dependent upon the particular measurements.

- The character of the radiation pattern seems to change with MLT in crossing from the post to pre-midnight periods. Data from the pre-midnight region indicates the possibility of only one area of more burst-like radiation, rather than the broad band precipitation, but with considerably harder, though highly variable, spectrums.
- Very little precipitation is observed near the magnetic pole.

The observations by an electron multiplier aboard Injun 3 of electrons on the night side with energies greater than 10 kev will not be discussed in this context because they occur generally during periods of large geomagnetic activity (Fritz and Gurnett, 1965; Fritz, 1967).

This criterion also pertains to the spikes of electrons with energies greater than 40 kev measured aboard Alouette 1 above the high latitude boundary of the outer belt (McDiarmid and Burrows, 1965). Of 37 events only two occurred for $K_p \leq 2+$.

On the other hand the electron microbursts detected by the Geiger counter aboard Injun 3, which had an energy threshold also at 40 kev, do not show a dependence of percentage occurrence upon the K_p value, at least in the region of maximum occurrence (Oliven et.al., 1968). These bursts appear to be a lower latitude phenomenon than the high latitude burst region of the kev energy electrons. They are primarily confined to invariant latitudes between 66° and 70° and morning magnetic local times from 0430 to 1230.

REFERENCES

Burch, J. L., Low-energy electron fluxes at latitudes above the auroral zone, J. Geophys. Res., 73, 3585, 1968.

Fritz, T. A., Spectral, spatial and temporal variations observed for outer zone electrons from 10 to 100 kev with satellite Injun 3, Ph.D. Thesis, Department of Physics and Astronomy, University of Iowa, 67-42, 1967.

Fritz, T. A., and D. A. Gurnett, Diurnal and latitudinal effects observed for 10-kev electrons at low satellite altitudes, J. Geophys. Res., 70, 2485, 1965.

Hoffman, R. A., Low energy electron bursts at high latitudes, (abstract), International Symposium on the Physics of the Magnetosphere, Washington, D. C., 1968.

Hoffman, R. A., and D. S. Evans, OGO-4 auroral particles experiment and calibrations, Goddard Space Flight Center preprint, X-611-67-632, 1967.

Hoffman, R. A., and D. S. Evans, Field aligned electron bursts at high latitudes observed by OGO-4, J. Geophys. Res., 73, 6201, 1968.

Johnson, R. G., R. D. Sharp, M. F. Shea and G. B. Shook, Satellite observation of two distinct dayside zones of auroral electron precipitation, (abstract), Transactions of the American Geophysical Union, 47, 64, 1966.

McDiarmid, I. B., and J. R. Burrows, Electron fluxes at 1000 kilometers associated with the tail of the magnetosphere, J. Geophys. Res., 70, 3031, 1965.

Oliven, M. N., D. Venkatesan, and K. G. McCracken, Microburst phenomena,

2. Auroral-zone electrons, J. Geophys. Res., 73, 2345, 1968.

Sharp, R. D., and R. G. Johnson, Satellite measurements of auroral particle

precipitation, To be published in Proceedings of the Advanced Study Institute

on Earth's Particles and Fields, Freising, Germany, 1967.

TABLE 1
CONVERSION FACTORS*

Bit Rate	0.7 kev Detector	7.3 kev Detector
4 kbps (Tape Storage Data)	6.70×10^5	8.13×10^4
16 kbps (Real Time Data)	2.68×10^6	3.25×10^5
64 kbps (Real Time Data)	1.07×10^7	1.30×10^6

*To convert from counts/readout to electrons/cm² -sec-ster-kev, multiply the counting rate by these factors.

FIGURE CAPTIONS

Figure 1. Responses of the 0.7 kev and 7.3 kev detectors to precipitating electrons in the northern hemisphere during a dusk to dawn polar crossing. ($K_p = 0+$).

Figure 2. Responses of the 0.7 kev and 7.3 kev detectors to precipitating electrons in the northern hemisphere in late morning. ($K_p = 2-$).

Figure 3. Four point energy spectrums of precipitating electrons. Data labeled "Band" were observed at about $70\frac{1}{2}^\circ$ invariant latitude during revolution 1099 on October 11, 1967. Data labeled "Burst" were observed at about 79° on the same revolution.

Figure 4. Data from the period labeled 'Expand' in Figure 2 from the 0.7 kev detector to illustrate the variability of the precipitating fluxes.

Figure 5. Responses of the 0.7 kev and 7.3 kev detectors to precipitating electrons in the northern hemisphere in very early morning. ($K_p = 2$).

Figure 6. Data from the period labeled "Expand" in Figure 5 from the 0.7 kev detector. These data are the highest time resolution data available from the satellite.

Figure 7. Responses of the 0.7 kev and 7.3 kev detectors to precipitating electrons in the northern hemisphere near midnight. ($K_p = 1-$).

Figure 8. The location in magnetic local time (MLT) and invariant latitude (Λ) of the band and burst regions. The curves labeled "A" show the

"Auroral Zone" and "Soft Zone" of Burch (1968) from data from the Aurora satellite. The curves labeled "L" are from a statistical study of the "centers of gravity" of the "hard" and "soft" zones reported by Sharp and Johnson (1967).

Figure 9. Pitch angle distribution for 2.3 kev electrons in the morning band during revolution 54. The average flux was 1.1×10^6 electrons/ $\text{cm}^2\text{-sec-ster-kev}$. The loss cone was calculated for an altitude of 100 km to remove all particles. The satellite was near perigee at 420 km altitude at $B = 0.431$ gauss and $L = 9.35$.

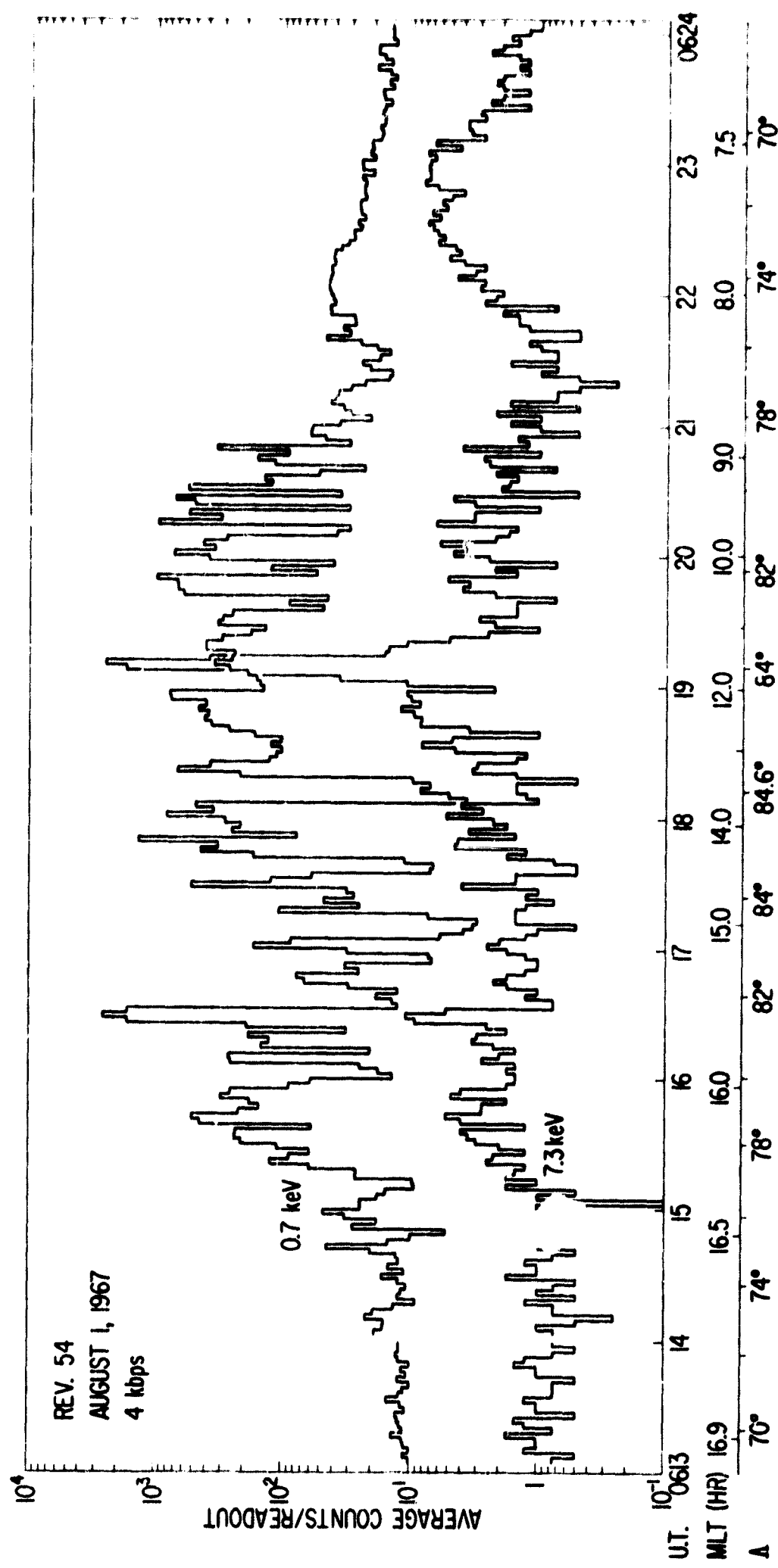


Figure 1

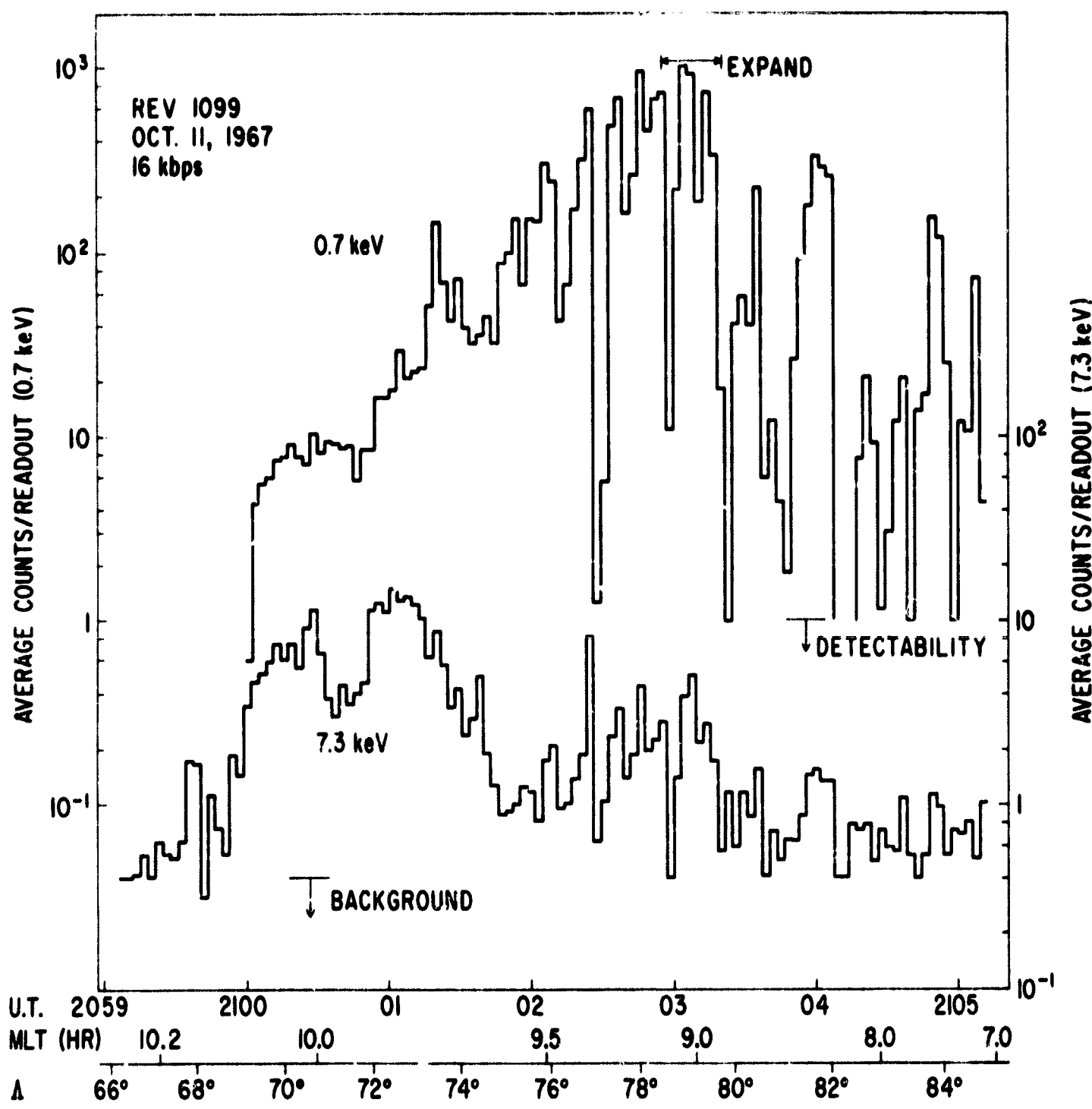


Figure 2

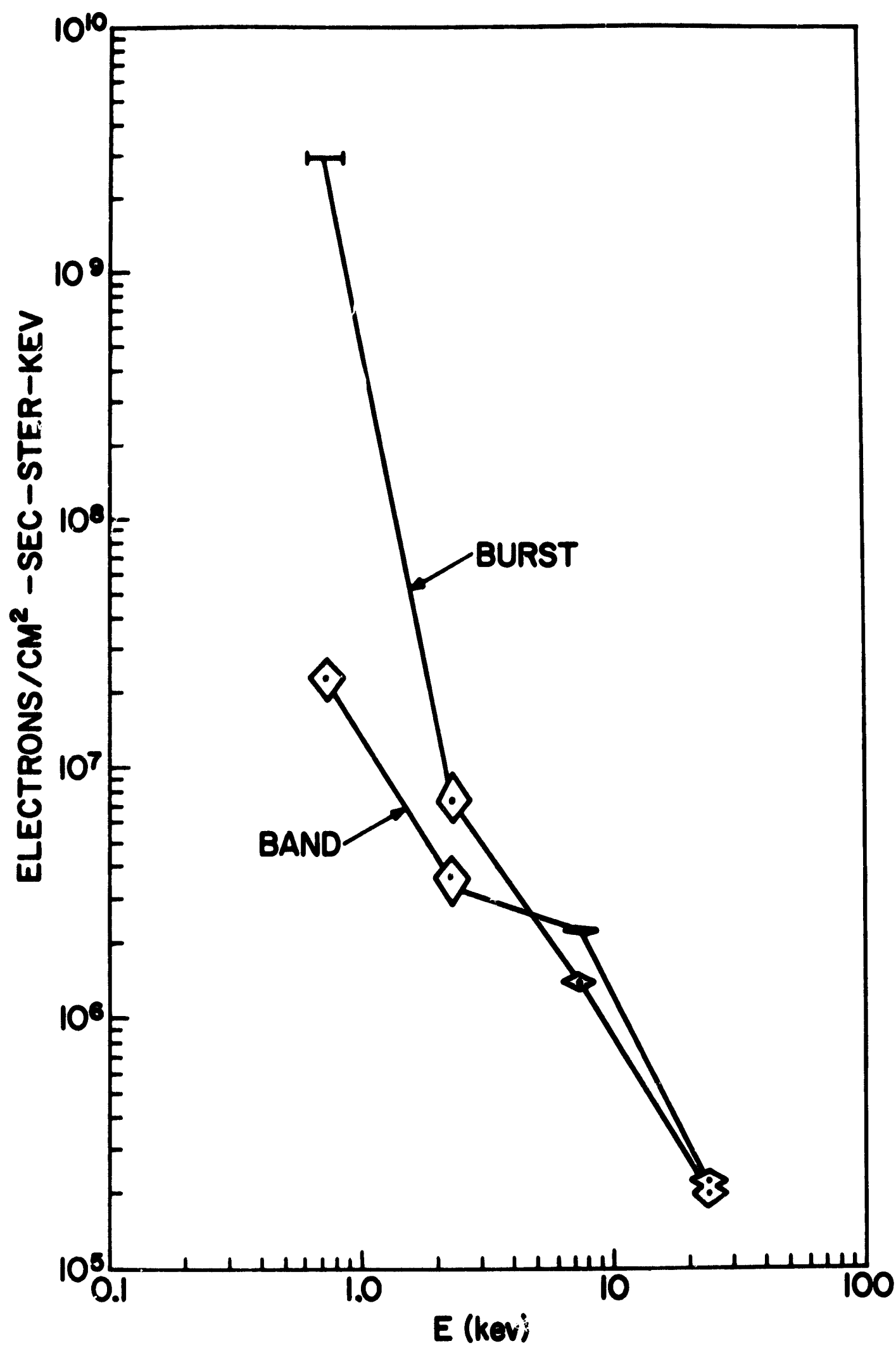


Figure 3

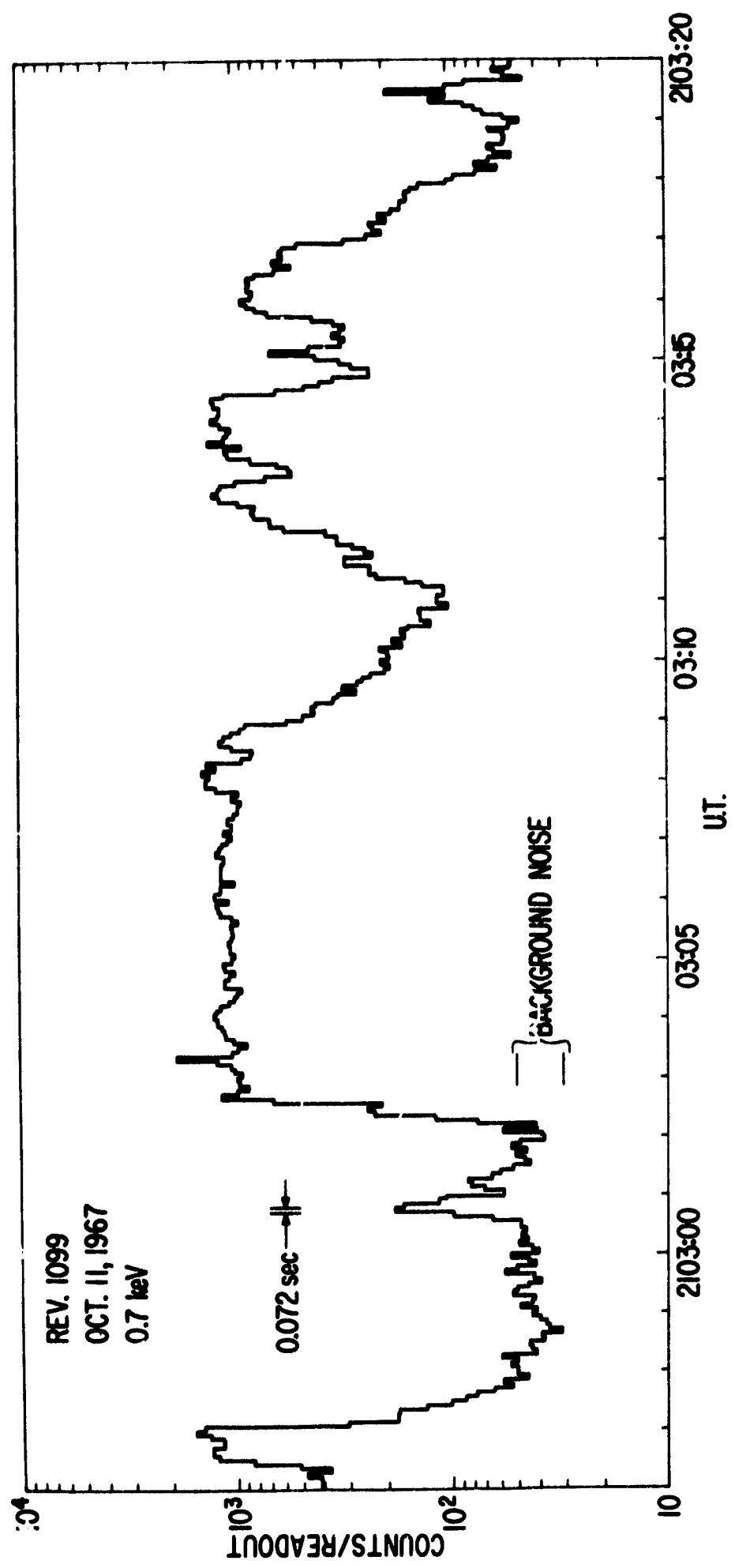


Figure 4

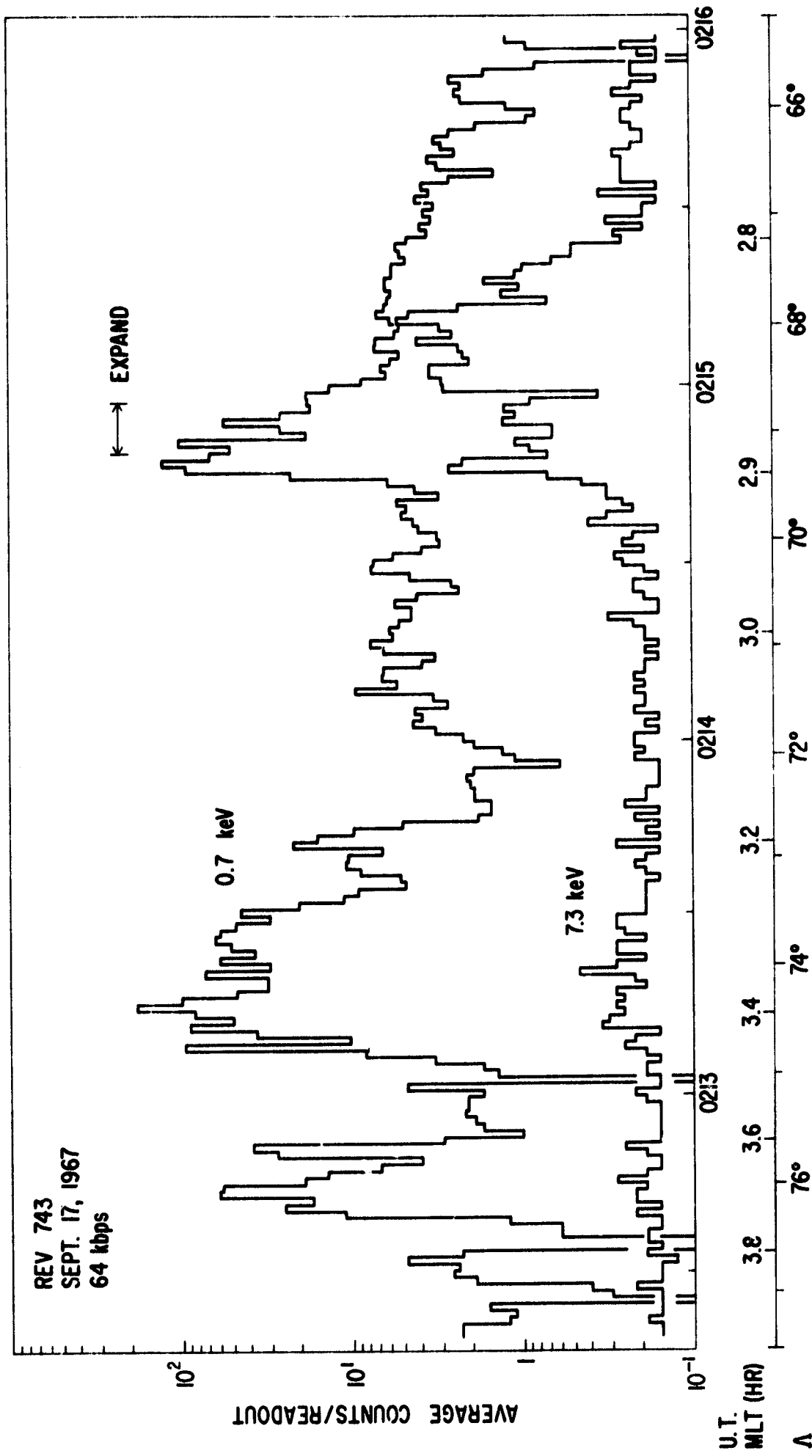


Figure 5

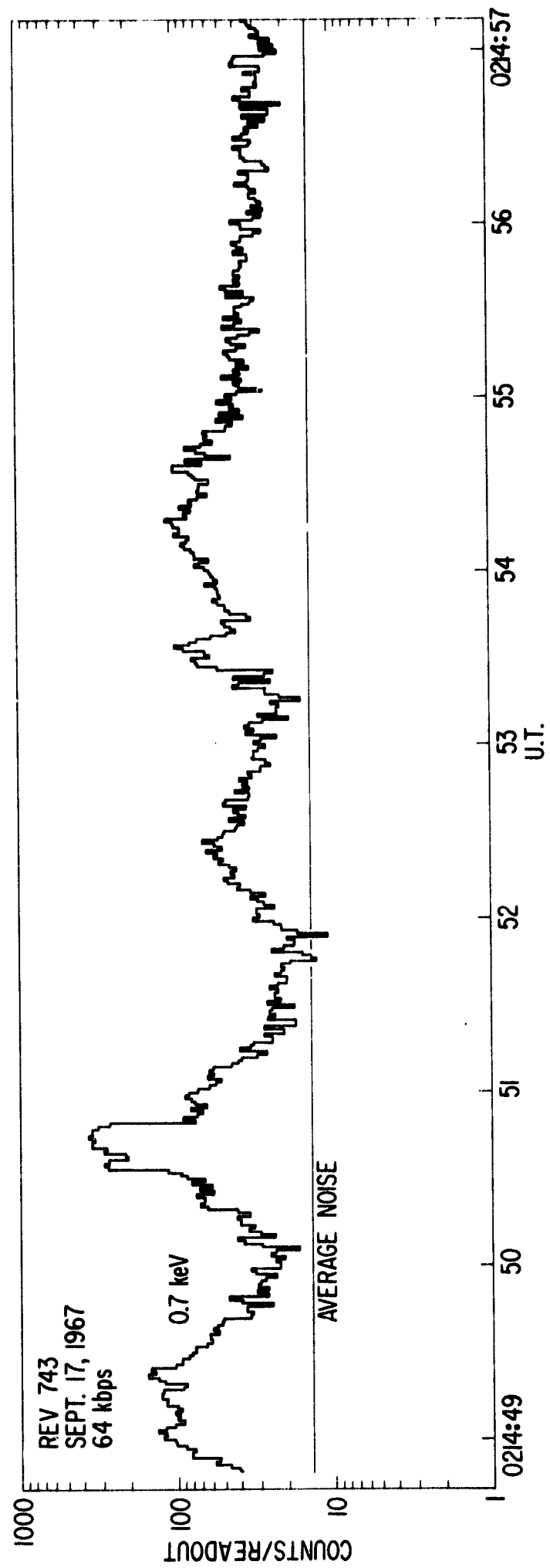


Figure 6

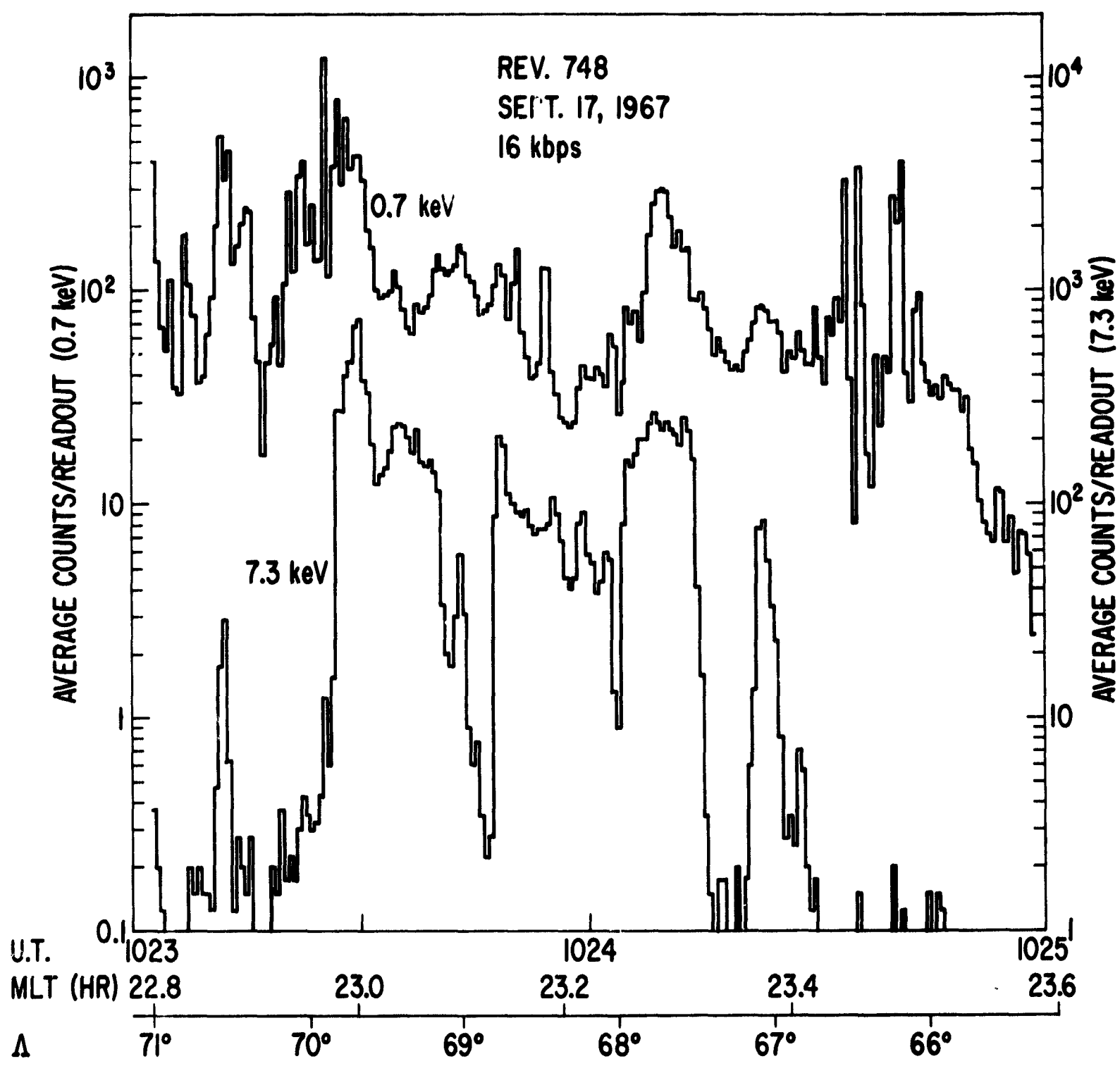


Figure 7

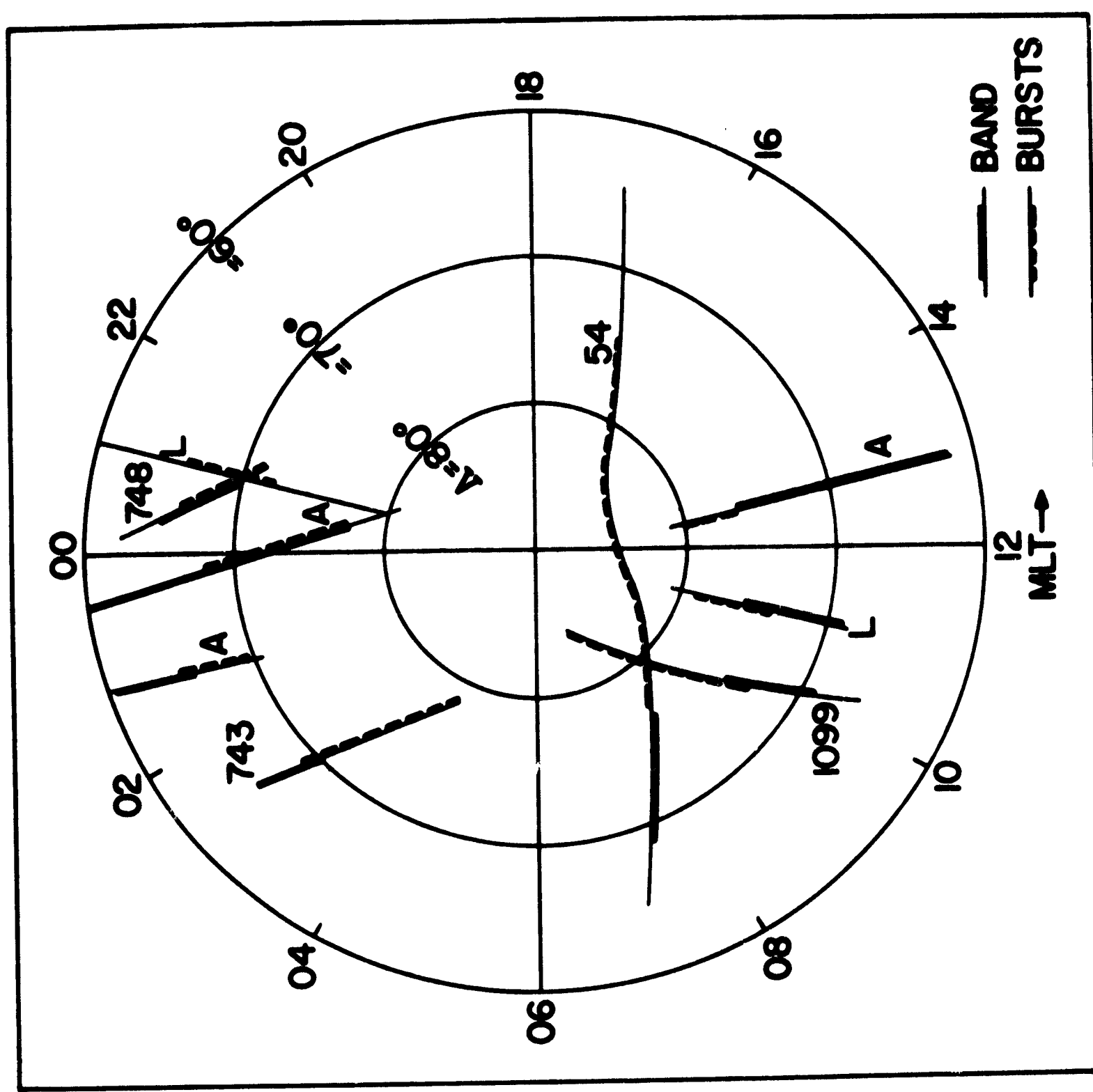


Figure 8

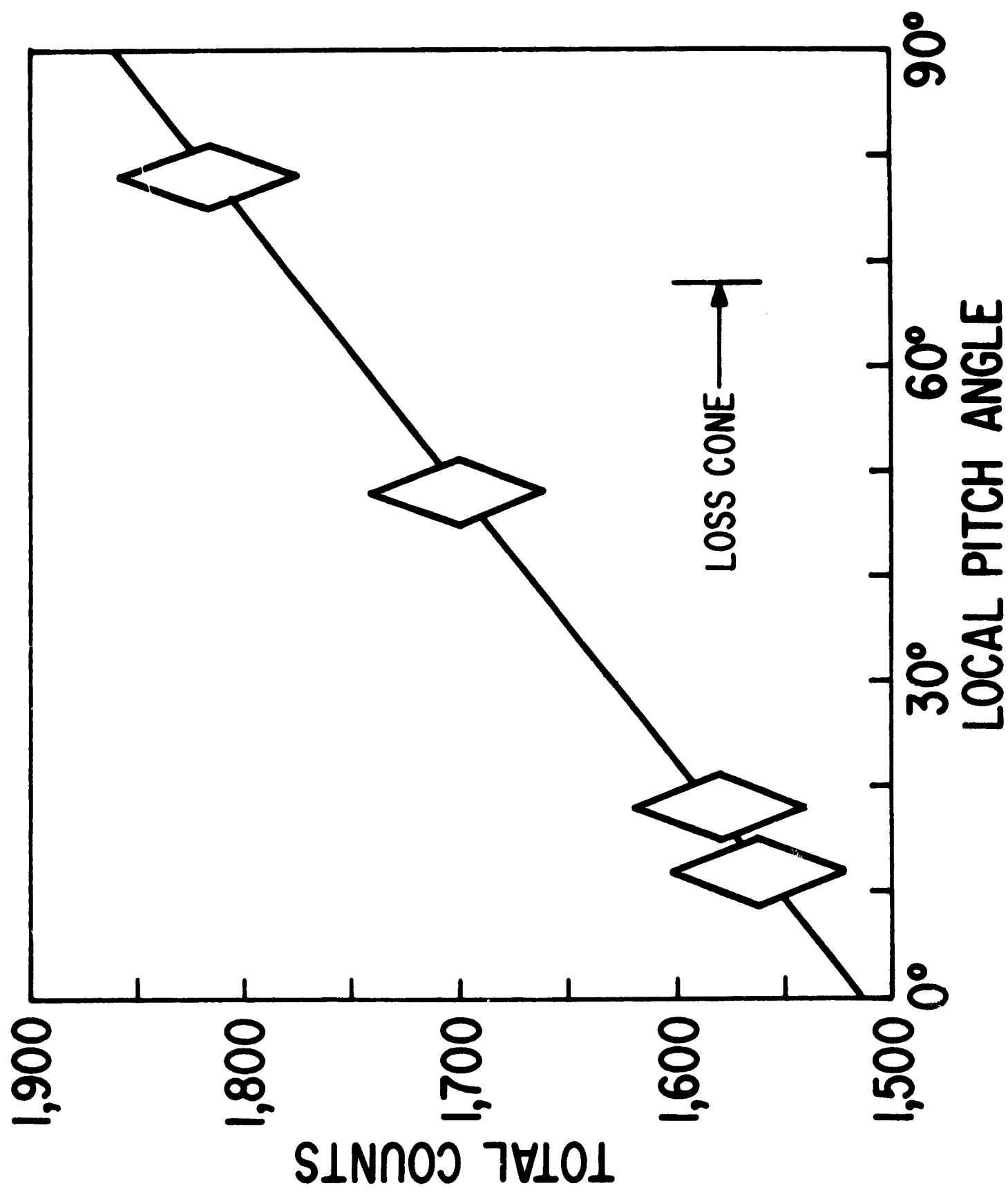


Figure 9